5th International Conference on Biaxial/Multiaxial Fatigue and Fracture
Cracow'97, Poland

T.S. GROSS[1], D.A. MENDELSOHN[2], and E.K. TSCHEGG[3]

Progress toward Understanding the Effect of Fracture Surface Interference on Shear Modes of Crack Growth

1. Department of Mechanical Engineering, University of New Hampshire, Durham, NH 03824 U.S.A.
2. Department of Aerospace Engineering, Applied Mechanics and Aviation, The Ohio State University, Columbus, OH, 43210 U.S.A.
3. Institute of Applied and Technical Physics, Technical University of Vienna, Karlsplatz 13, A 1040 Wien, Austria

Keywords: Shear modes, fracture surface interference, crack tip shielding, modeling, experimental evidence

ABSTRACT: The modeling and experimental work to determine the effect of fracture surface interference on the driving force for shear crack growth is reviewed.

Introduction

Shear and mixed modes of crack growth are a significant component in multiaxial fatigue crack growth, fracture of tough materials, fracture of composites and other anisotropic materials, failure of turbogenerator shafts, and rolling contact fatigue to name a few. There is question as to whether the success of linear elastic fracture mechanics in predicting Mode I crack can be applied to Mode II and Mode III crack growth. It is thought that the interference of the opposing fracture surface asperities shield the crack tip from the applied stresses. The resistance to applied shear is related to the normal force that results from the crack faces being wedged open as the asperities are displaced relative to one

another in shear. If this effect is significant, the success of fracture mechanics for prediction of shear crack growth depends on incorporation of the effect of fracture surface interference in the expressions for the driving force for shear crack growth.

The following is a summary of our view of the state of understanding of the effect of fracture surface interference on shear crack growth. First, we present a physical picture of how crack faces might interact. Then, we briefly describe the effect simplifying assumptions have on the predictions of the models of crack face interactions. Following that, a brief summary of the experimental evidence of crack tip shielding by fracture surface interference is presented. Finally, we present recent estimates of crack face tractions during shear obtained using a hybrid analytical-experimental approach.

Fig. 1 Schematic representation of the single point contact (left) and distributed contact (right) interaction in a semi-infinite edge crack under remote shear load τ with resulting resistance and normal loads, F_a, N_a or F, N, are resolved to the asperity plane or the macroscopic crack plane, respectively.

The basic questions

There is little disagreement that fracture surfaces are at least microscopically rough. Depending on how the crack grows, the asperities may or may not be interdigitated on the micrometer or finer scale, but are definitely matching and interlocked on a sub-millimeter and above scale. Therefore, as the opposing crack faces are displaced relative to one another in shear, the asperities can either ride up on one another, can smear one another, or they can deform in compression. If the asperities ride up on one another, the opening is resisted by the elastic hinge of the remaining ligament resulting in a normal traction on the opposing asperities. If they deform or smear, then there is some roughly constant opening that results in a constant normal traction. The questions are:

- What are the magnitudes of the shear and normal tractions?
- How are they related to one another?
- At what normal and/or shear stress do the asperities smear or deform?
- How do the tractions depend on applied load?

Modeling

The simplest picture of the crack face interaction is that deduced from analysis of an interlocking sawtooth shown in Figure 1. Ballarini and Plesha (1) and Mendelsohn and Gross (2) both used Coulomb friction applied across an inclined asperity and then resolved the resultant forces parallel to and perpendicular to the macroscopic crack plane to calculate the shear and opening tractions. Evans and Hutchinson (3) took a similar approach for a kinked crack at a bimaterial interface. The macroscopic resistance to the applied shear stress, F_r, is related to the normal contact stresses, N_c through;

$$F_r = \Gamma N_c$$
$$\Gamma = \frac{\mu + \tan\alpha}{1 - \mu \tan\alpha} \qquad (1)$$

where Γ is the crack face interaction parameter and is a function of the angle of inclination of the asperity, α, and the coefficient of friction, μ. This approach assumes that the opening and shear tractions are coupled.

Linear elastic fracture mechanics allows the superposition of the applied and resistance stress intensity factors to calculate the effective stress intensity factor. If one knows the pressure distribution, $\sigma(r)$, on the crack faces, Rice(4) has shown that the stress intensity factor can be calculated from;

$$K_I = \sqrt{\frac{a}{\pi}} \int_0^{r=a} \frac{\sigma_C(r)dr}{\sqrt{1-r^2}}$$
$$K_{IIR} = \sqrt{\frac{a}{\pi}} \int_0^{r=a} \frac{\sigma_R(r)dr}{\sqrt{1-r^2}} \qquad (2)$$

where a is the crack length, r is the distance from the crack tip, σ_C is the normal contact stress distribution, σ_R is the resistance shear stress distribution.

If one assumes single point contact, then the resistance stress intensity factor can be calculated assuming $\sigma(r)$ is a Dirac delta function. The normal force at r_c, the contact point, is a function of the opening, $u_{op}(r_c)$. Assuming that the opening displacements follow a classical $\sqrt{r}$ displacement law and that the Irwin plastic zone model describes crack tip displacements, the resistance stress intensity factor can be estimated from;

$$K_{IIR} = \Gamma\left(\frac{E \bullet u_{op}(r_c)}{4(1-\nu^2)}\right)\sqrt{\frac{2\pi}{r_c + r_y}}$$
$$r_y = \frac{K^2_{Iind}}{\pi\sigma_{ys}} \qquad (3)$$

where σ_{ys} is the yield stress, r_y is the plastic zone radius, E is the elastic modulus, K_{Iind} is the induced Mode I stress intensity factor, and ν is Poisson's ratio. This approach was applied to estimate the resistance stress intensity factor for an actual Mode I fatigue crack profile (5) The upper and lower faces of a digitized profile were shifted to generate an effective Mode II stress intensity factor. The Mode II resistance SIF (Equation 3) was calculated from the normal force required to open the crack faces so that they were

contacting at a single point. The shifted profiles are shown in Figure 2 and the applied Mode II SIF required to generate an effective Mode II SIF is shown in Figure 3.

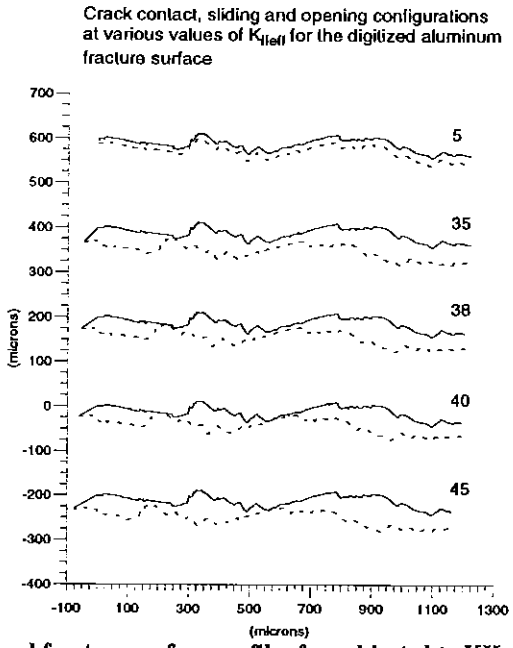

Fig. 2 Shifted digitized fracture surface profiles for subjected to KIIeff where the profiles opened so that there was single point contact.

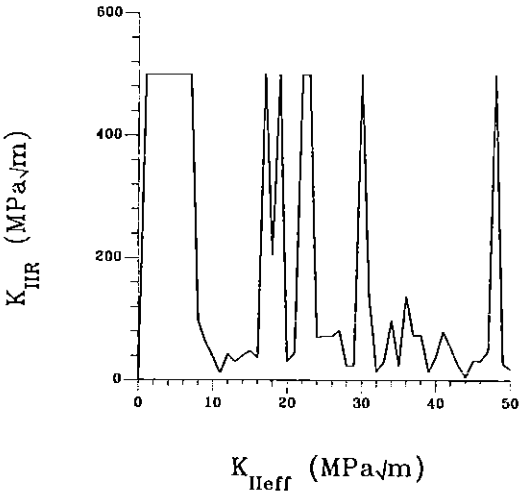

Fig. 3 Resistance stress intensity factor vs effective stress intensity factor assuming single point contact for steel.

Clearly, the resistance is extremely high (>100 MPa$\sqrt{m}$) and the assumptions of the model make it too stiff to be consistent with the experimental observations of Mode II and Mode III fatigue crack growth. However, the high resistance does explain why Mode II and Mode III crack growth are not typically observed. The normal and shear forces are more than sufficient to cause compressive yielding of the asperities which would reduce the normal and therefore the resistance forces. The primary question that cannot be definitively answered by modeling is, how much do the asperities yield and/or smear?

Distributed contact over the entire crack face is the opposite extreme to point contact. Ballarinni and Plesha (1) assumed that the opening displacements are proportional to the shear displacements through the sawtooth asperity angle and that the frictional resistance is proportional to the normal contact stress through the interaction coefficient, Γ. For no crack tip yielding, this approach yields a resistance that is linearly proportional to the applied Mode II or Mode III stress intensity factor.

In an attempt to simulate smearing and include crack tip plasticity, Gross and Mendelsohn (6) proposed that the interlocking and sliding applies only up to a maximum shear displacement, λ_c, and that, for greater shear displacements, $\Gamma = \mu$, the friction coefficient. This transition results in an order of magnitude decrease in resistance for a given opening. In addition, the normal contact stresses were not allowed to exceed the yield strength. When the displacements over the entire crack face were less than λ_c, the resistance was proportional to the applied shear just as for Ballarini and Plesha. The rate of increase in resistance with applied shear decreased as the portion of the crack face that exceeded λ_c approached the tip. A large decrease in resistance results when the crack face displacements are all greater than λ_c. The magnitude of the resistance was shown to increase with increasing crack length, coefficient of friction, asperity angle, and yield strength. Asperity amplitudes of 50 μm or less produced resistance stress intensity factors that were a substantial fraction of the applied stress intensity factor.

For reasonable materials properties and range of fracture surface roughness, the modeling indicates that fracture surface interference can substantially shield the crack tip from the applied shear loading. The major uncertainty is how much of the crack face is in contact and how much and when the asperities deform.

Experimental evidence

The strongest experimental evidence that the fracture surface asperities interfere is from the fractographic observation of Mode III monotonic and fatigue fracture surfaces (7). The circumferentially notched cylindrical specimens are typically precracked in Mode I cyclic compression. The Mode III portion of the fracture surface inevitably exhibits smeared or fractured asperities. A "factory roof" fracture surface consisting of approximately millimeter amplitude, radially oriented, alternately inclined facets, is often observed for fatigue crack growth in steel to greater fractions of the diameter. An example of these features can be seen in Figure 4.

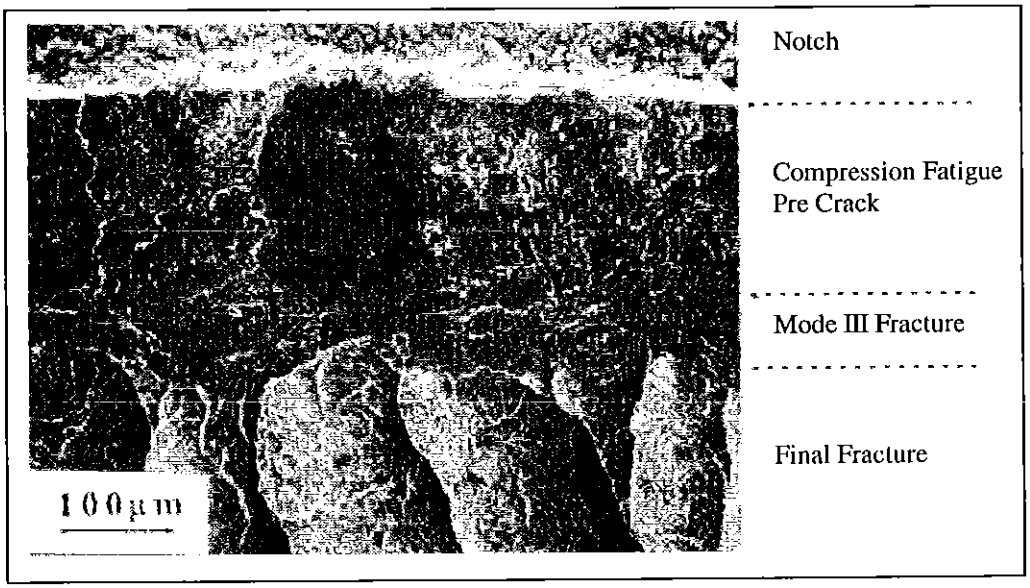

Fig. 4 Scanning electron fractography showing the precrack region, Mode III fracture surface and final fracture regions.

Aside from the fact that shear modes of crack growth are rarely observed, Mode II and Mode III crack initiation and growth is usually observed only at higher stresses. It is proposed that this occurs because the interlocking component of the fracture surface interference is only overcome by the applied shear when there is some smearing or compressive deformation of the short wavelength asperities. Crack initiation under cyclic torsion was observed to occur on the planes of maximum cyclic shear only for higher stress amplitudes. The cracks initiated normal to the principal stress direction for lower stress

amplitudes (8,9). Another observation that supports the notion that the asperities must be smeared for shear crack growth to occur is that most observations of Mode II crack growth occur for growth rates exceeding micrometers per cycle (9). These high crack growth rates usually correspond to moderately high stresses.

In the early 1980's, Mode III crack growth from torsionally loaded, circumferentially notched specimens received considerable attention especially by author #3. Several papers showed that the Mode III fatigue crack growth rate decreased with increasing crack length even though the applied Mode III stress intensity factor (or plastic strain intensity, Γ_{III}) was held constant (10-12). This violation of similitude was attributed to interference of the fracture surface asperities and was termed, sliding crack closure. An example of this behavior is shown in Figure 5. Assuming similitude does apply for shear crack growth, the "interference free" Paris law constants can be estimated by extrapolating this data to zero crack length. Figure 6 shows the crack length dependence of the resistance stress intensity factor, ΔK_R, implied by the data in Figure 5 assuming $da/dN = C(\Delta K_{app} - 2\Delta K_R)^m$. The resistance is roughly linearly dependent on crack length. It increases with increasing K_{IIIapp} (with the exception of the 60 MPa$\sqrt{m}$ data which violates the small scale yielding criteria for this sample). Although this effect has weaker experimental support because only three data points were used to determine C and m in the Paris law. The fracture surfaces in these specimens were inevitably smeared even with a superimposed Mode I loading.

Frictional resistance is always proportional to the normal force whether it is sliding or sliding and interlocking. For shear cracks, the normal force is proposed to originate from the elastic "hinge" of the remaining ligament. For the "hinge" to exert a force, it must be opened. Therefore, any fracture surface resistance must be accompanied by crack face opening. Several instances of induced crack face opening under remote, pure shear loading have been reported in the literature. Figure 7 shows an extreme case for a wood composites (Parallam, particle board, and solid wood) in which the crack mouth opening displacements are in excess of millimeters (13). For metals, the crack mouth opening displacements have been observed to be on the order of tens of micrometers for 10-20 mm cracks [14]. The opening displacements persist to or near the tip as long as there are crack face shear displacements. So, crack face opening induced by asperity interference during shear is an experimentally documented fact.

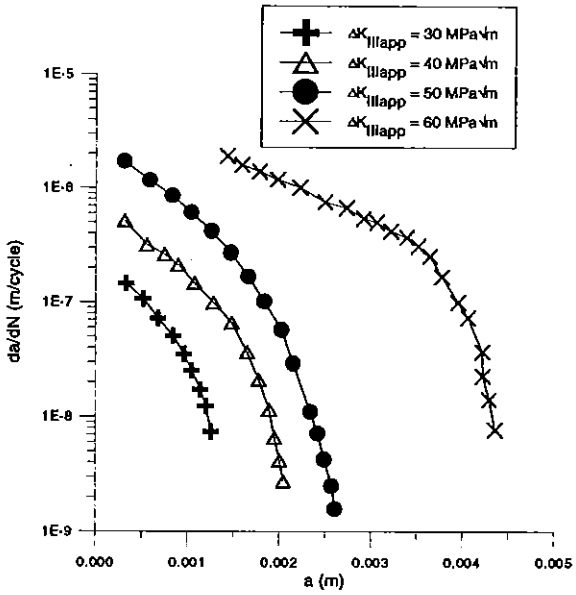

Fig. 5 Mode III fatigue crack growth rate as a function of crack length at constant applied ΔKIII. Note the violation of similitude.

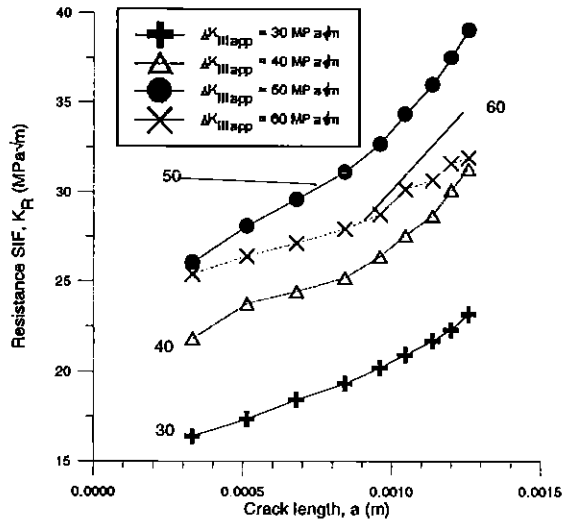

Fig. 6 Resistance stress intensity factor implied by the reduction of da/dN in Figure 6

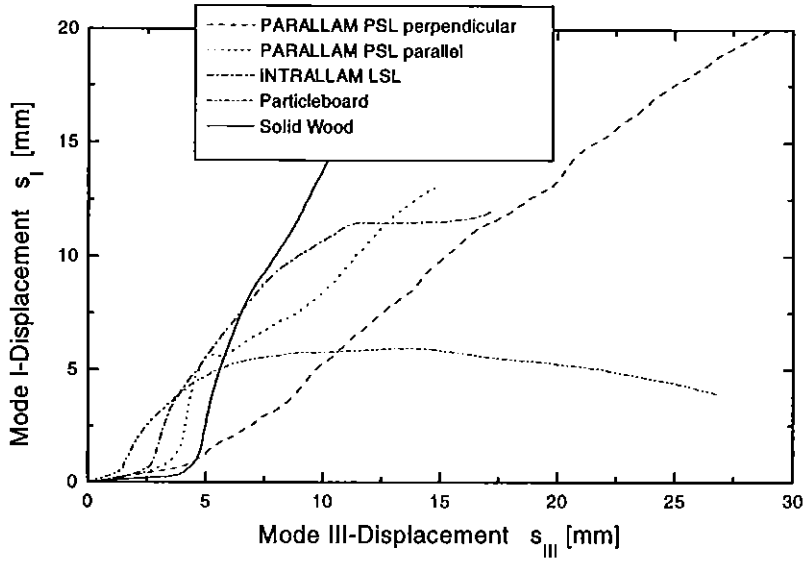

Fig. 7 Mode I crack opening as a consequence of the rough crack surface (no external mode I load).

The resistance stress intensity factor, K_R, can be determined from the difference between the applied and effective stress intensity factors. Goulet (15) estimated the effective Mode II stress intensity factor, K_{IIeff}, and induced Mode II stress intensity factor, K_{iind}, from interferometric measurements of the crack displacement field. He studied the effect of yield strength and elastic modulus on the dependence of K_R on K_{IIapp} for two steels and 7075 Al. The data is shown in Figure 8 and 9. In both the aluminum and the steel, the lower strength material exhibited low K_R (~2 MPa$\sqrt{m}$) that was roughly constant. In contrast the higher strength materials exhibited locking for K_{IIapp} < 6-8 MPa$\sqrt{m}$. After overcoming the initial locking, the K_R was roughly constant at 6-8 MPa$\sqrt{m}$ or slightly decreasing for the 7075-T6 aluminum. The K_R continued to increase with K_{IIapp} to 10-12 MPa$\sqrt{m}$ for the 4340 steel. Goulet suggested that the K_{IIapp} at breakaway and the magnitude of the roughly constant resistance after breakaway both increase with increasing yield strength-to-modulus ratio.

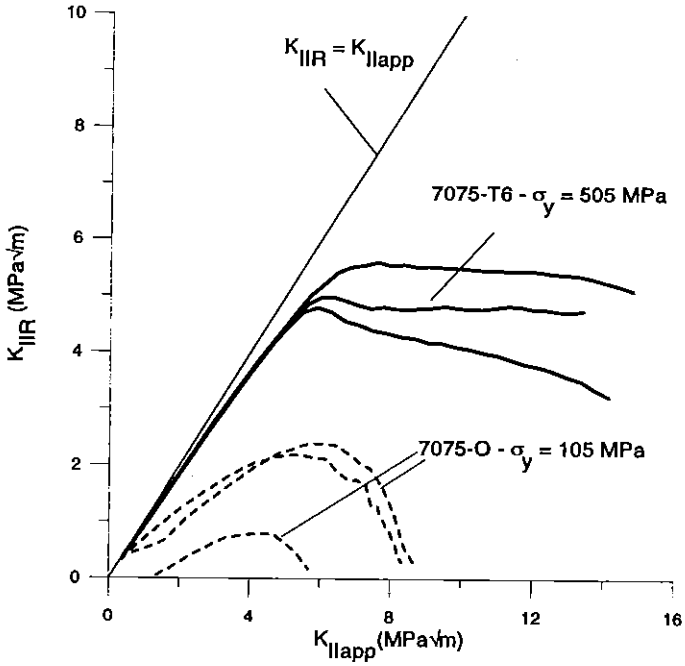

Fig. 8 Resistance stress intensity factor vs applied stress intensity factor for two aluminum alloys. Note the lower strength has less resistance.

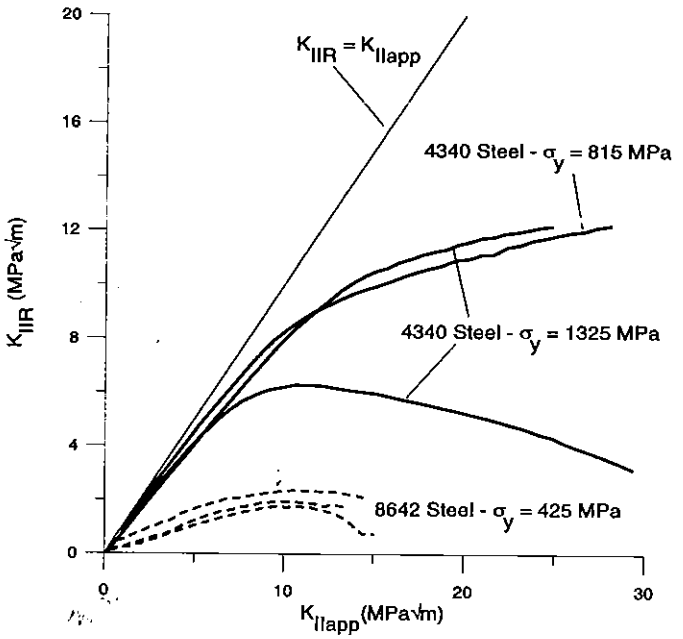

Fig. 9 Resistance stress intensity factor vs applied stress intensity factor for two steel alloys. Note the lower strength has less resistance.

The crack face tractions were deduced by using the experimentally obtained crack face shear and opening displacement field as a crack face boundary condition in a linear elastic with Dugdale strip yielding, boundary element model of the specimen. Figure 10 shows the shear and normal tractions as a function of distance from the tip for a 4340 steel ($R_c = 45$). The normal stresses are roughly constant for a distance of 2-4 mm from the tip of the 12 mm long crack. Near the tip and for $r > 6$ mm, the crack faces are not in contact. The ratio of the shear resistance to the normal contact stress, Γ, in Figure 12 shows that the state of contact changes as a function of distance from the tip. The regions of higher Γ near the tip are attributed to interlocking. Further out, it is proposed that the short wavelength asperities have smeared and the crack faces are riding up long wavelength, shallow slope asperities.

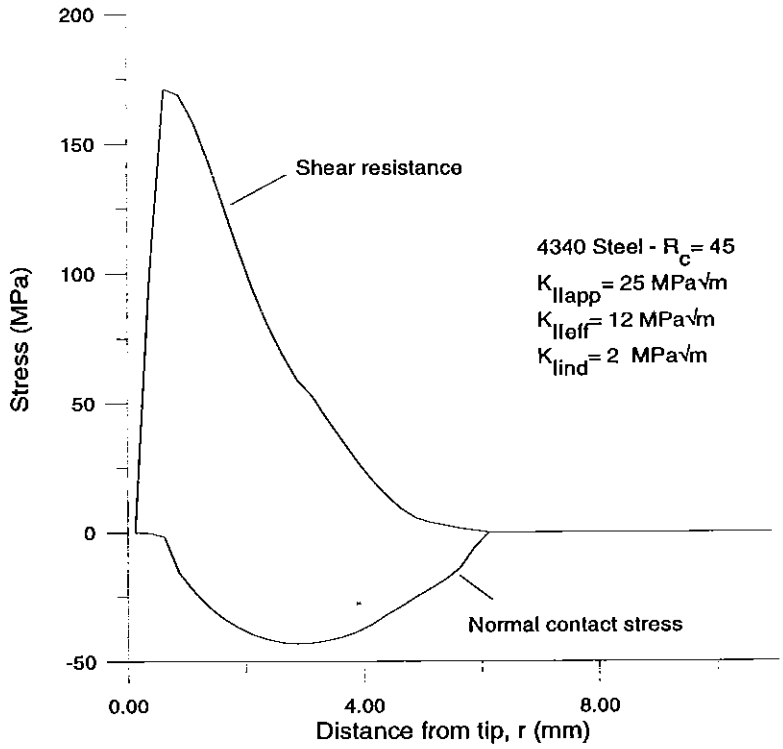

Fig. 10 Contact stress distributions inferred from experimentally observed crack face shear and opening displacement profiles.

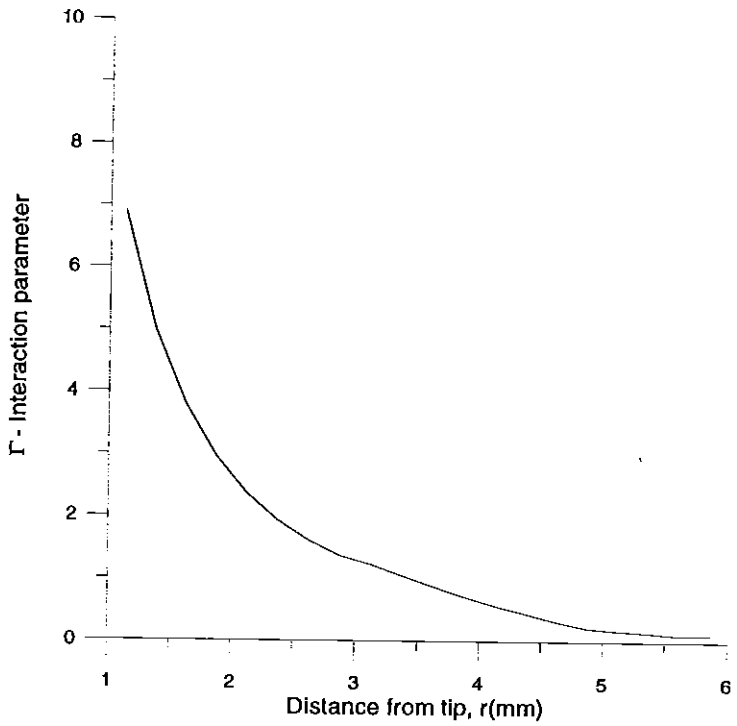

Fig. 11 Interaction parameter inferred from Figure 10.

Summary

Fracture surface interference clearly has an effect on the rate and driving force for shear crack growth. That the crack faces are wedged open as they are displaced in shear is an experimentally established fact. The yield strength to elastic modulus ratio affects the K_{IIapp} at which the transition from locking to sliding occurs. A hybrid experimental-analytical estimate of the crack face tractions suggest a changing state of contact along the crack face where large portions of the crack are not in contact.

References

(1) BALLARINI, R. and PLESHA, M., (1987), The effects of crack surface friction and roughness on crack tip stress fields, Int. J. Frac., vol. 34, pp. 195-207

(2) GROSS, T.S. and MENDELSOHN, D.A., (1988), On the effect of crack face contact and friction dut to fracture surface roughness in edge cracks subjected to external shear, Eng. Frac. Mech., pp. 405-420

(3) EVANS, A.G. and HUTCHINSON, J.W., (1989), Effects of non-planarity on the mixed mode fracture resistance of bimaterial interfaces, Acta Met. Vol. 37, pp. 909-916

(4) RICE, J.R., (1968), Fracture: An Advanced Treatise - Vol. II, Ed. H. Leibowitz, Academic Press, New York, NY, pp. 214-223

(5) MENDELSOHN, D.A., GROSS, T.S., and ZHANG, Y.,(1995), Fracture surface interference in shear -I. A model based on experimental surface characterization, Acta Metall. vol. 43, pp. 893-900

(6) GROSS, T.S. and MENDELSOHN, D.A., (1989), Mode I Stress Intensity factors induced by fracture surface roughness under pure Mode III Loading: Application to the effect of loading modes on stress corrosion crack growth, Metall. Trans, vol. 20A, pp. 1989-1999

(7) TSCHEGG, E.K. and SURESH, S., (1988) Mode III fracture of 4340 steel: Effects of tempering temperature and fracture surface interference, Metall. Trans., vol 19A, pp. 3035-3044

(8) RITCHIE, R. O., McCLINTOCK, F.A., NAYEB-HASHEMI, H., and RITTER, M.A., (1982), Mode III crack propagation in low alloy steel, Metall. Trans., vol. 18A, pp. 101-110

(9) LIU, H.W., (1985), Shear Fatigue Crack Growth: A Literature Survey, Fat. Frac. Eng. Mat. Str., vol. 8, pp. 295-313

(10) TSCHEGG, E.K., STANSZL-TSCHEGG, S.E., (1988), The significance of sliding mode crack closure on mode III fatigue crack growth, Basic Quest. In Fatigue, ASTM STP 924, (Edited by J.T. Fong and R.J. Fields), vol. 1, pp. 214-232

(11) TSCHEGG, E.K., (1983), Sliding mode crack closure and Mode III fatigue crack propagation in mild steel, Acta Meta., vol. 31, pp. 1323-1330

(12) TSCHEGG, E.K., (1982), A contribution to Mode III fatigue crack propagation, Mat. Sci. Eng., vol 54, pp. 127-137

(13) EHART, R.J.A., TSCHEGG, E.K., STANSZL-TSCHEGG, S.E., (1997), Mode III fracture energy of wood composites in comparison to solid wood, Wood Sci. Technol., in press

(14) GOULET, R.U., GROSS, T.S., and MENDELSOHN, D.A., (1996), Evidence of fracture surface interference for cracks loaded in shear using phase shifted speckle intereferometry, Metall. Trans, vol. 27A, pp. 3853-3860

(15) GOULET, R.U., (1997), An experimental investigation of the effects of elastic modulus and yield strength on fracture surface interference in shear loaded cracks, Ph.D. Thesis, University of New Hampshire, U.S.A.